Underground Mining Technology 2017 – M Hudyma & Y Potvin (eds)

doi:10.36487/ACG_rep/1710_16_Carusone

Variations in apparent stress and energy index as indicators of stress and yielding around excavations

O Carusone *Laurentian University, Canada*

M Hudyma *Laurentian University, Canada*

Abstract

Analysis of source parameters of microseismic events provides useful information about the rock mass response to mining. Energy index and apparent stress are source parameters that quantify relative co-seismic stress adjustment. Trends in these parameters might show how mining-induced stresses change in the initial hours after a blast. Analysis of events following production blasts in a deep open stoping operation suggests that the rock mass undergoes a rapid stress increase immediately after the blast, followed by some degree of more gradual yielding. These responses vary between different stope blasts and spatially around a stope. These results may also vary with local conditions such as rock mass properties and stoping geometry.

Keywords: *seismic monitoring, rock mass response*

1 Introduction

A well-maintained seismic monitoring system has a multitude of applications beyond providing locations and magnitudes of events. With adequate data quality, microseismic events can provide useful information on the response of the rock mass to mining. Analysis and interpretation of trends in seismic source parameters can help provide such information. The goal of this study is to examine trends in seismic source parameters linked to co-seismic stress, and relate them to rock mass response around open stopes.

Rock mass response from stope blasts can be placed into two broad categories: a stress increase from the newly formed excavation, or some degree of stress decrease because the rock mass begins to yield or is stress shadowed. The latter may be preceded by a stress increase which induced the subsequent yielding. Hudyma et al. (1994) present readings from strain cells near a 5,000 tonne stope blast which are shown in Figure 1. Both strain cells indicated a large stress increase in the first few minutes after the blast. In the following hours, the strain rate on cell #1 (Figure 1(a)) exhibited a slow increase, eventually reaching equilibrium, while the strain on cell #9 (Figure 1(b)) began to decrease and level off at a point higher than the pre-blast reading. Strain cell #1 was located farther from the stope, where the ground was still elastic, while strain cell #9 was located closer to the stope, near a zone that began to yield following the stope blast. These two basic responses are what was believed to be present in microseismic data.

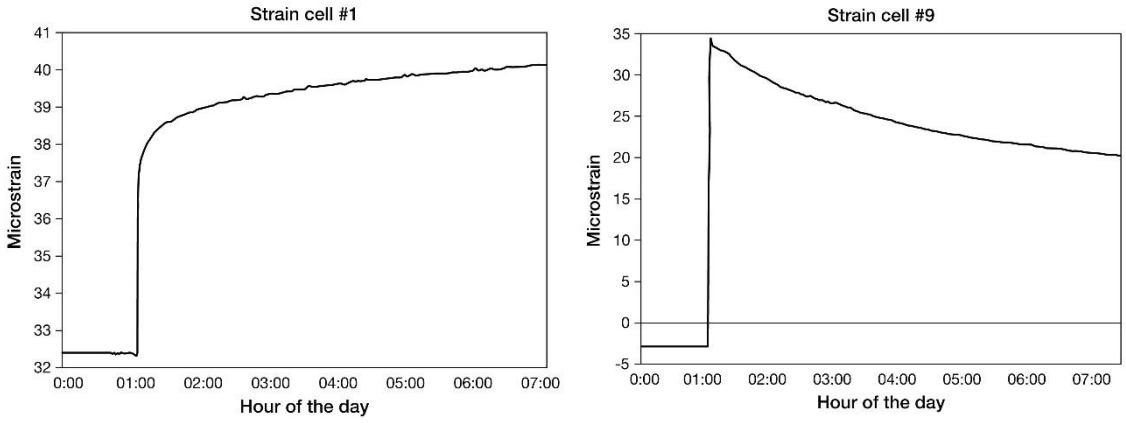

(a) (b)

Figure 1 Strain cell readings following a 5,000 tonne stope blast 50 m (a); and 30 m (b) from the stope (Hudyma et al. 1994)

The mine in this study is a deep copper–nickel mine in the Sudbury Basin. The mine uses transverse blasthole open stoping in a primary-secondary sequence. The stopes measure 30 m tall by 12.5 m along strike, and are up to 30 m in length (across strike). After access and raise bore development, stopes are taken in two blasts: a toe slash that breaks the bottom 10 m of the stope into the undercut, and a final which takes the remaining 20 m and daylights in the overcut. Blasts of this size rapidly induce large stress changes ,and seismic responses, as the rock mass adjusts to the loss of confinement and redistribution of stress around the new void.

Data was collected using an ESG Solutions Paladin® microseismic array with over 50 sensors, including 19 15Hz triaxial geophones. Sensors are located in the hanging wall and footwall of the orebody, which improves both location and source parameter accuracy by providing more complete coverage of the event focal sphere. Events were located with a median error residual of 2.6 m, and site personnel manually pick at least five triaxial geophones for events larger than moment magnitude -1. The database has been manually cleared of blasts, and checked for consistency of source parameter estimates over the studied period.

2 Interpretation of rock mass behaviour using microseismic events

Stress–strain behaviour in a rock mass can be inferred from microseismic events. If the events are consistently well-located, the behaviour can be linked to a specific volume of rock. This study focused on two parameters and analyses techniques: energy index and apparent stress. Energy index (EI) is a comparison of an event's radiated energy to the average energy radiated by an event with the same moment, based on the energy–moment scaling relation of a population of events. Moment (M) is a proxy for co-seismic rock mass deformation. Events with larger moments involve larger displacements over larger areas (Aki & Richards 1980). Events with higher radiated energy for the same moment (higher EI), would occur where more strain energy is stored in the rock, and thus suggest a higher level of stress. The inverse of this relation can also help describe a relative increase in strain in a rock mass. If an event has a higher moment for the same radiated energy, it has a lower EI and implies more movement occurred (van Aswegen & Butler 1993). These concepts are illustrated in Figure 2.

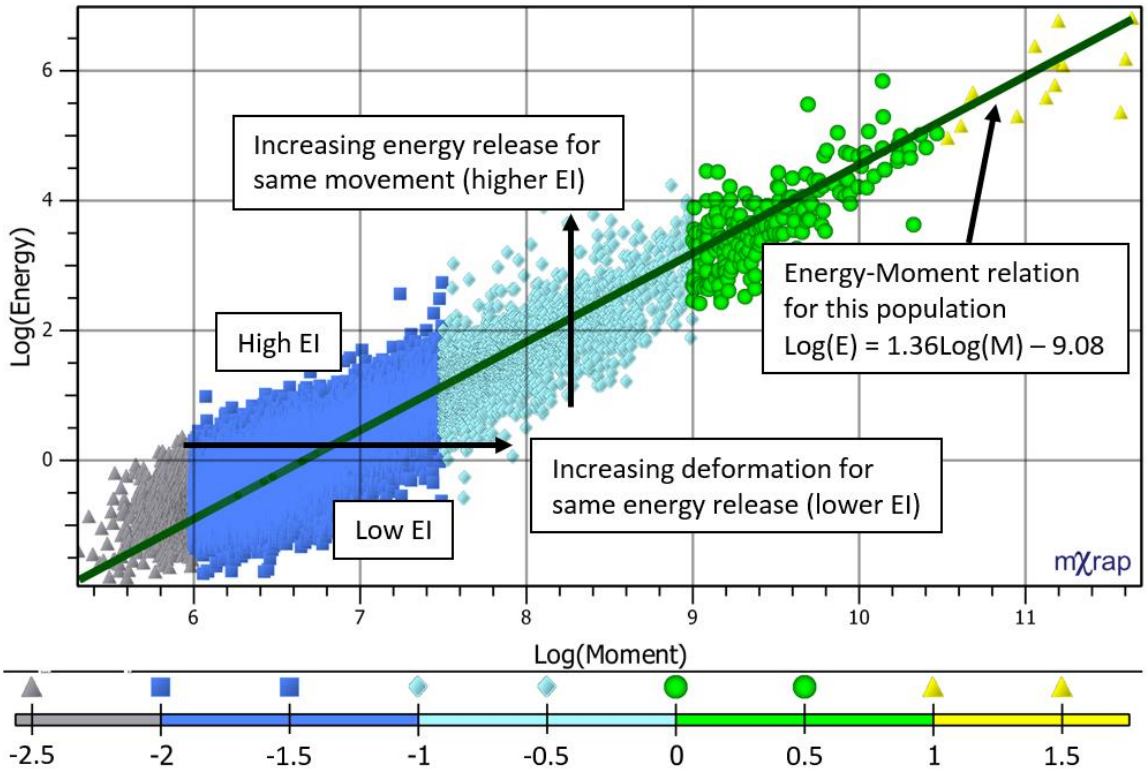

Figure 2 Example of an energy (E)–moment (M) relation with events coloured by moment magnitude

On an event-by-event basis, EI is a highly volatile parameter, so it is often tracked as a moving average or median to show longer term trends (e.g. Glazer & Hepworth 2006; Mendecki et al. 1999). In this study, Log(EI) is tracked to further smooth out trends. The calculation for Log(EI) modified from Mendecki et al. (1999) is shown in Equation 1. The best fit for energy–moment relations was determined using a quantile–quantile relationship in the software mXrap (Harris & Wesseloo 2015). The procedure for determining the best fit is outlined in Wesseloo et al. (2014). Because of the power-law nature of seismic events, EI trends inevitably show the behaviour of small events rather than larger ones, which may affect interpretation of stress–strain behaviour (Hudyma 2008).

$$\log(EI) = \log\left(\frac{E_{Obs}}{E_{Exp}}\right) = \log(E_{Obs}) - [d \times \log(M_{Obs}) + c] \quad (1)$$

where:

E_{Obs} = observed radiated energy.

E_{Exp} = expected radiated energy for observed seismic moment based on energy–moment relation.

M_{Obs} = observed seismic moment.

c = intercept of energy–moment log relation (Figure 2).

d = slope of energy–moment log relation (Figure 2).

Apparent stress (σ_a) is a seismic source parameter that is indicative of the relative stress change associated with a seismic event. The parameter is based on the energy and moment of the seismic event, and the shear modulus of the rock mass. Apparent stress after Wyss and Brune (1968) is calculated using Equation 2 and illustrated on an energy–moment relation in Figure 3. Events with higher apparent stress occur in higher stress conditions and in stronger, more intact ground (Brown & Hudyma 2017a; Simser & Falmagne 2004). Apparent stress is scale dependent in this dataset, meaning that, typically, larger events will have higher apparent stress than smaller ones. This scale dependence is what separates EI from σ_a. While such scale dependence is a point of contention revolving around the self-similarity of earthquakes (or lack

thereof) and limitations of instrumentation bandwidth (e.g. Ide & Beroza 2001), the scaling of apparent stress with moment in this dataset may still prove useful for interpretation of stress–strain behaviour. Apparent stress is determined through:

$$\sigma_a = \frac{\mu E}{M} \tag{2}$$

where:

μ = shear modulus of the rock mass.

E = radiated energy of the event.

M = seismic moment of the event.

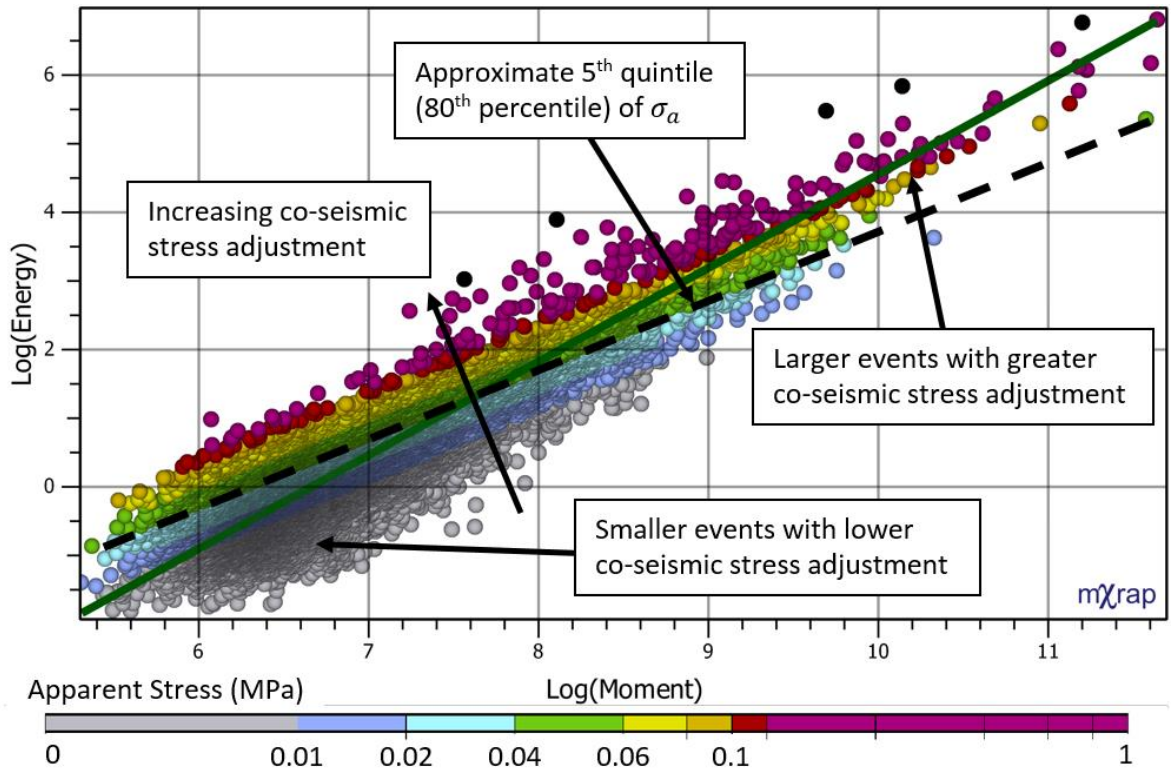

Figure 3 Example of an energy–moment relation with events coloured by apparent stress (modified from Alcott et al. 1998)

Time histories of apparent stress have previously involved tracking the average rate of events over a given threshold (e.g. Hudyma 2008; Young 2012). Such methods were not applied in this study because the frequency of high apparent stress events would not directly indicate the level of relative co-seismic stress change. Apparent stress has also been tracked using the upper and lower quintile and ratio between quintiles in a moving time window (e.g. Brown 2015; Brown & Hudyma 2017b). These methods may be more applicable to describing a level of relative co-seismic stress change.

3 Methodology for tracking trends

EI and σ_a were tracked using a moving window of the last 200 events. A window of 200 events was found to be long enough to produce a stable trend, but short enough to show how the characteristics of events can rapidly change in the hours following a stope blast. A moving window of the number of events was used instead of a fixed time window to reduce the influence of time artefacts. Time artefacts occur when a group of events that occurred over a short time period and caused a large, sudden change in a trend line leave the moving window and make it appear as if another sudden shift has occurred. Using a fixed number of events will not eliminate an artefact, but it might make the change slightly less abrupt. Another way to

avoid the effect of artefacts might be to use discrete 'blocks' of 200 events. This method would eliminate the effect of artefacts from events leaving the moving window, but would reduce the temporal resolution at which we can interpret the trends.

EI and σ_a were tracked in similar manner to previously cited works in Section 2. Log(EI) was tracked as a moving average, and σ_a was tracked as a moving 5th quintile (80th percentile) referred to as AS_{80}. While different methods of normalising these parameters and smoothing their trends may reveal different behaviours, comparing the results and potentially different interpretations drawn from by previously published methods is also of interest. Comparing log-normalised versus un-normalised parameters or smoothing trends with other techniques (e.g. averages, medians, quintiles, etc.) may produce other interesting or useful results, but is beyond the scope of this study. The trend lines used nearby events, prior to the stope blasts, to establish initial levels of Log(EI) and AS_{80}.

Only events within 50 m of the final stope void were analysed. This spatial restriction on the analysed events ensured that the trends in relative co-seismic stress change were influenced by local conditions rather than events that occurred elsewhere under different rock mass conditions.

Energy index for all events was calculated using the same energy–moment relation: Log(E) = 1.335 Log(M) – 8.783. This relation was determined from approximately 300,000 M_w > -2.5 events detected throughout the mine over a six year period. The purpose of using a consistent energy–moment relation was to be able to draw relative comparisons in EI between the different blasts without potential influence of varying energy–moment relations over space and time. A more detailed study might investigate the use of energy–moment relations more specific to the location of the blast or the time around which it occurred. Different energy–moment relations might change the observed EI trend and affect our interpretation of rock mass behaviour.

4 Observed trends

Trends in Log(EI) and AS_{80} were analysed for 50 stope blasts which ranged between 7,000 and 35,000 tonnes. The analysed blasts were selected because they had the most events larger than M_W -1.5 occurring within six hours of the blast and up to 60 m from the blast centroid. The blasts had between approximately 150 and 650 events larger than M_W -1.5. Blasts that induced greater numbers of seismic events potentially involved greater stress change. Potential for greater stress change coupled with the greater quantity of data for drawing trends made these blasts the most attractive subjects for analysis.

The majority of trends in both EI and σ_a had similar characteristics to the stress cell readings in Figure 1(b). Forty-two of the Log(EI) trends and 49 of the AS_{80} trends began with a rapid increase immediately after the blast followed by a more gradual decrease. While blasts are characterised by high EI and σ_a, these non-events have been cleared from the dataset, and are therefore not the source of the initial increase in Log(EI) or AS_{80}. A gradual climb following the drop was also observed in 41% of the cases for Log(EI), and 48 of the cases for AS_{80}. This third phase was not analysed in great detail because it was not always clear when the influence of the blast-related seismicity ended and seismicity from other sources, such as stope mucking or stress change from nearby blasts, began to take over the trend. Both Log(EI) and AS_{80} exhibited a sudden increase followed by a more gradual decrease in 41 of the analysed cases. A typical example of this behaviour following a 30,000 tonne stope blast is shown in Figure 4. The stope blast in this example induced over 1,000 events in the first two hours after the blast. Different phases of relative co-seismic stress change are indicated on the graph.

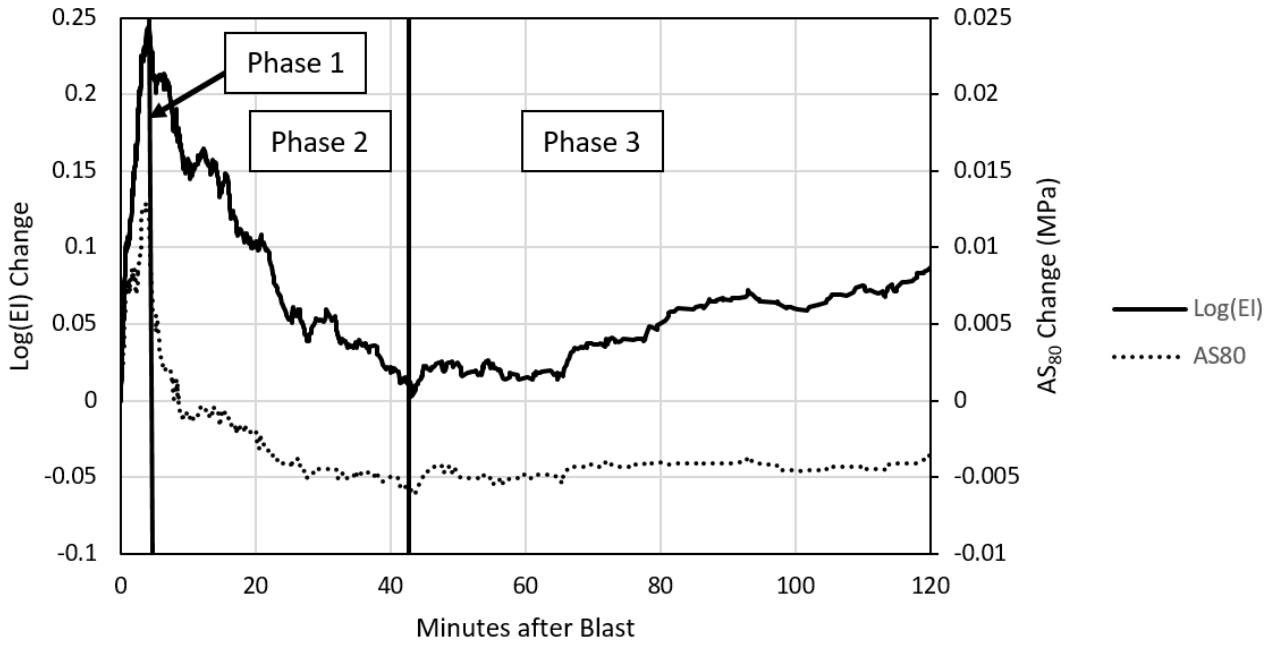

Figure 4 Example of most commonly observed behaviour following analysed stope blasts

The eight Log(EI) trends and single AS_{80} trend that did not fit the typical case exemplified in Figure 4 started with a gradual decrease. These cases are peculiar because localised stress increases following blasts are expected, but a decrease in either Log(EI) or AS_{80} implies a stress decrease. A typical example of this behaviour is shown in Figure 5. A stress increase may be occurring, but the dominant seismic response is one of decreasing relative co-seismic stress change. The 7,700 tonne blast induced 230 events that caused Log(EI) to drop and level off 50 minutes after the blast.

None of the analysed blasts exhibited an immediate decrease in both Log(EI) and AS_{80}. This result highlights how these different methods of tracking relative co-seismic stress change may lead to different interpretations of rock mass behaviour. The cases with an immediate decrease did not have pre-blast levels of Log(EI) or AS_{80} that were consistently higher or lower than those of the cases that exhibited an immediate increase. The most notable commonality between cases with this behaviour is the tonnage of the blast. An immediate decrease in either trend was found in nine out of 20 stope blasts smaller than 17,000 tonnes.

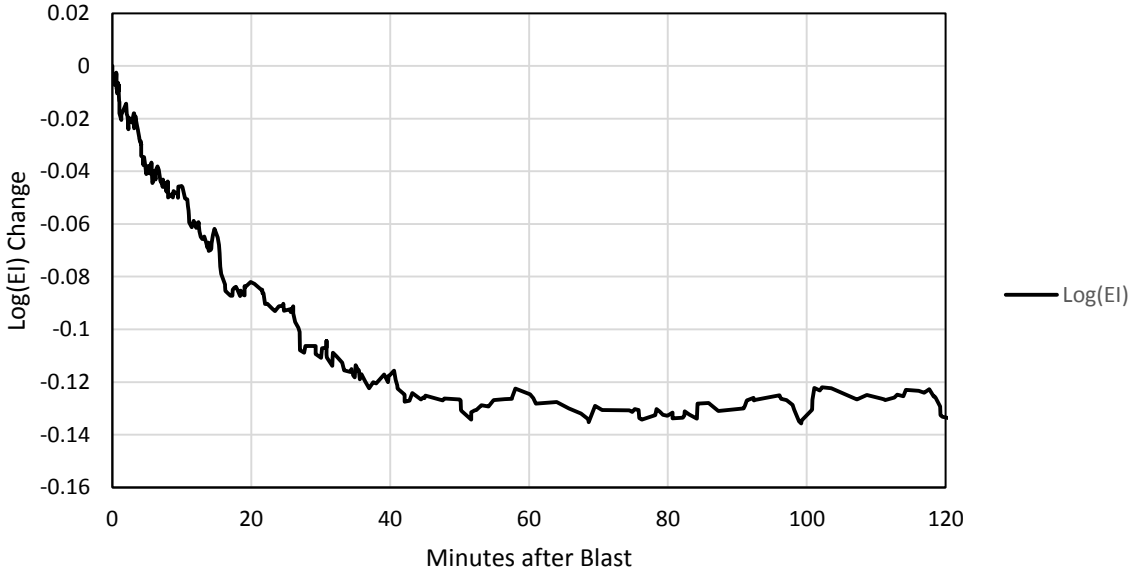

Figure 5 Example of Log(EI) trend that decreases immediately after a stope blast

The remainder of the analysis was focused on the first two phases of the 41 cases where both Log(EI) and AS_{80} underwent a rapid increase after the blast, followed by a more gradual decrease. On average, phase 1 lasted 6.2 minutes in Log(EI) trends, and 3.9 minutes in AS_{80} trends. Phase 2 lasted 100 and 90 minutes on average for Log(EI) and AS_{80} respectively. While phase 1 was relatively short, it consisted of 135 events on average, so the changes during this phase are believed to be significant.

Figure 6 compares the magnitude of change in Log(EI) to the magnitude of change in AS_{80} for phases 1 and 2. A larger change in one trend will generally coincide with a large trend in the other, but AS_{80} will sometimes exhibit a much larger change relative to the change in Log(EI). Differences in duration and relative magnitude of increases/decreases in the two trends indicate that there might be scale dependence in energy variation following the blasts. The energy–moment relation may not be simply translating up and down (changing vertical axis intercept). The slope of the relation and variance in seismic energy for a given moment may also be changing. This result demonstrates that using a single seismic source parameter or measure of central tendency or distribution may not reveal the full picture of how relative co-seismic stress change is varying.

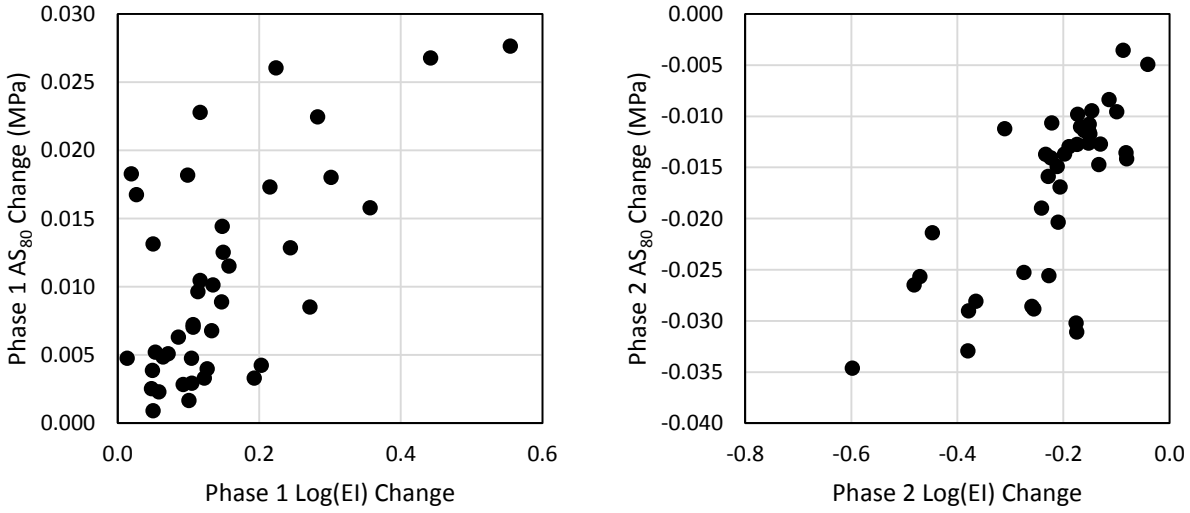

(a) (b)

Figure 6 Change in Log(EI) compared to change in AS_{80} in phases 1 (a); and 2 (b)

Figure 7 compares the magnitude of increase during phase 1 to the magnitude of decrease during phase 2 for both Log(EI) and AS_{80}. In general, a larger increase during phase 1 was met with a larger decrease during phase 2. This result demonstrates that there is some consistency in the behaviour with increasing scale of relative co-seismic stress change. From this, we might infer that larger initial stress increases result in larger stress decreases as the rock mass yields. No strong correlation was found between the magnitude of increase or decrease in either parameter and the duration of either phase.

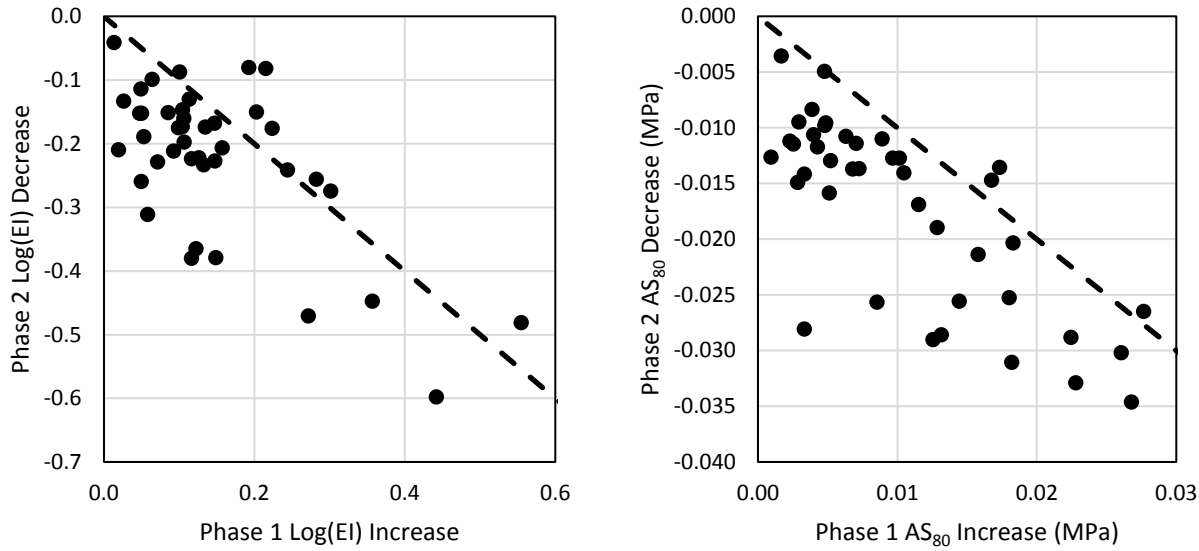

(a) (b)

Figure 7 Increase during phase 1 compared to decrease during phase 2 for Log(EI) (a); and AS_{80} (b)

For both parameters, the increase during phase 1 was usually smaller than the decrease during phase 2. If the decrease in either trend is interpreted as the decrease in stress as the rock mass yields, then these results are partially in contradiction to those of Hudyma et al. (1994). The strain cell readings in Figure 1(b) levelled off at a point higher than the pre-blast levels despite the instrument being located in yielding ground. However, more seismic events typically occur closer to newly formed excavations (e.g. Syrek & Kijko 1988). Trends in Log(EI) and AS_{80} will be influenced by greater quantities of events with more consistent and drastic variation in EI and σ_a. Because more events occur closer to the stope, and if we assume that the ground near to stope undergoes greater yielding and stress decrease, it is possible that the overall trend is dominated by the nature of events occurring in closer proximity to the stope. The strain cell that produced the readings in Figure 1(b) was 30 m away from an open stope. If the instrument was located closer to the void, Hudyma et al. 1994 may have observed an overall decrease in stress. This analysis also does not consider the gradual increase in Log(EI) and AS_{80} during phase 3. The levels of Log(EI) and AS_{80} at the end of this phase may provide a more complete representation of relative co-seismic stress change and inferred stress increases/decreases following stope blasts.

4.1 Spatial variations in trends

With sufficient data, individual trends for different areas around a stope can be identified, which increases the spatial resolution at which we can interpret rock mass behaviour. Between different volumes of rock, trends in Log(EI) and AS_{80} can vary in terms of:

- Duration of phases.
- Scale of increases/decreases (absolute and relative to other phases).
- Overall shape of trend (i.e. fit to examples presented in Figures 1, 4, and 5).
- Agreement between Log(EI) and AS_{80} trends.

The following example demonstrates how spatially filtering groups of seismic events can highlight differences in inferred rock mass response around the stope. The events in this example occurred after a 20,000 tonne stope blast that increased the stope height by 20 m and daylighted the overcut. The locations of the events and spatial groups around the stope are shown in Figure 8. Group A is located in the back of the recently blasted stope, while groups B and C are located in the walls.

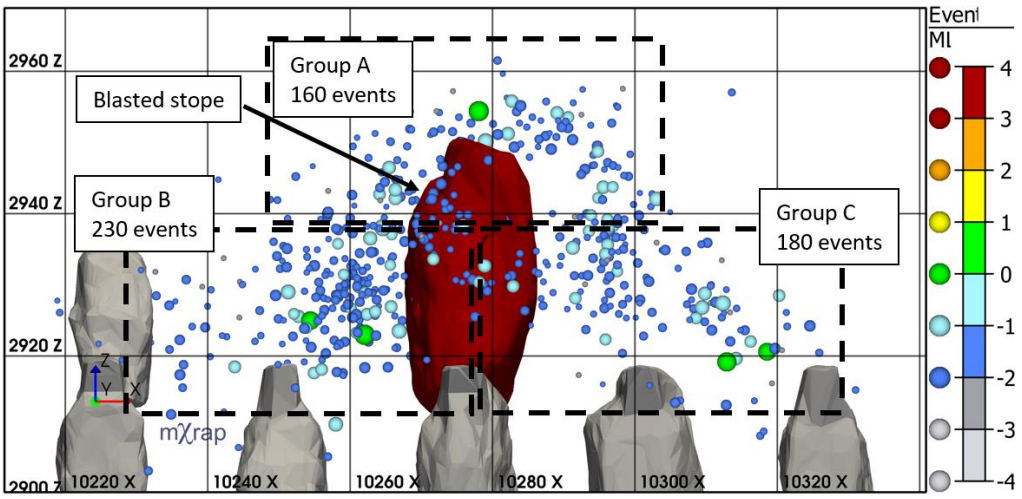

Figure 8 Seismicity in two hours following a stope blast. Events are coloured and sized by moment magnitude

Firstly, it should be noted that each spatial group has a different starting point for Log(EI) and AS_{80}, which implies that there are already significant spatial differences in relative co-seismic stress change before the blast was taken. Groups A, B, and C had an AS_{80} of 39, 30, and 41 kPa, respectively. Initial levels of Log(EI) for groups A, B, and C were 0.30, 0.22, and 0.29, respectively.

Figures 9 and 10 show the change in Log(EI) and AS_{80} in each individual group and the overall trend for all groups. Overall, the combined groups fit our most typical case of rapid increase followed by more gradual decrease. However, each individual group exhibits distinct behaviour from the others. Groups A and C both begin with an increase in Log(EI) and AS_{80}, but group A's trend lines began to drop after around 20 minutes, while group C's remained elevated similar to the strain cell readings presented in Figure 1(a). Group B exhibited a fairly consistent decrease in Log(EI) and only a small initial increase in AS_{80} before a slow, consistent drop over the next couple of hours.

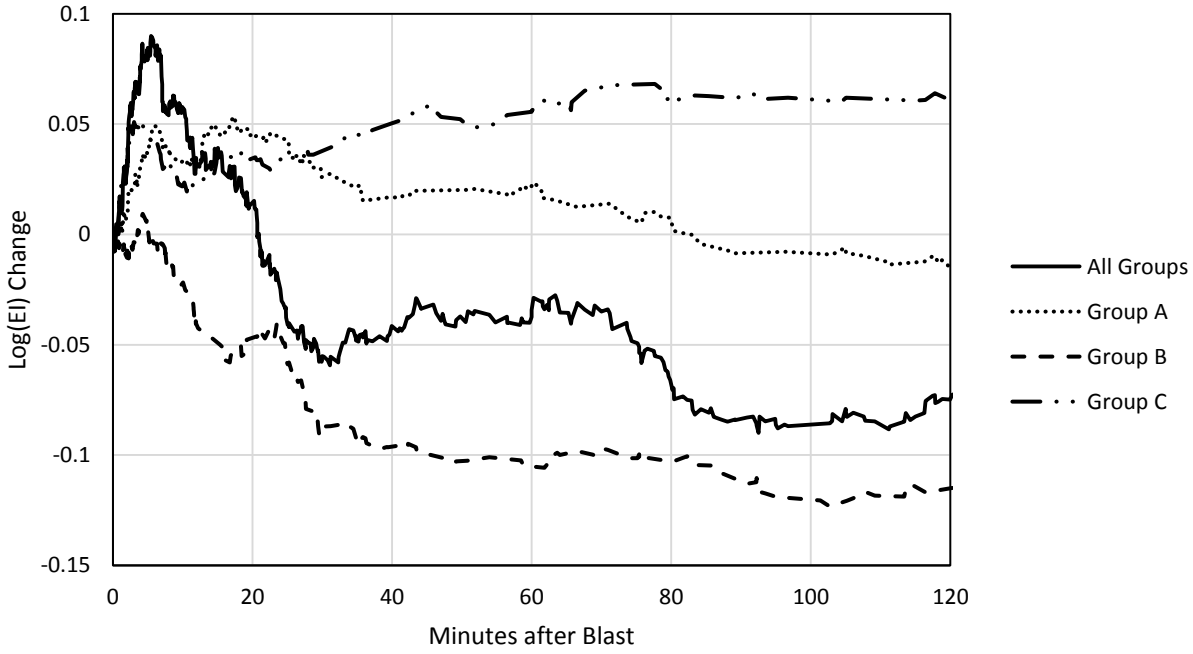

Figure 9 Changes in Log(EI) for spatially filtered groups around a stope blast

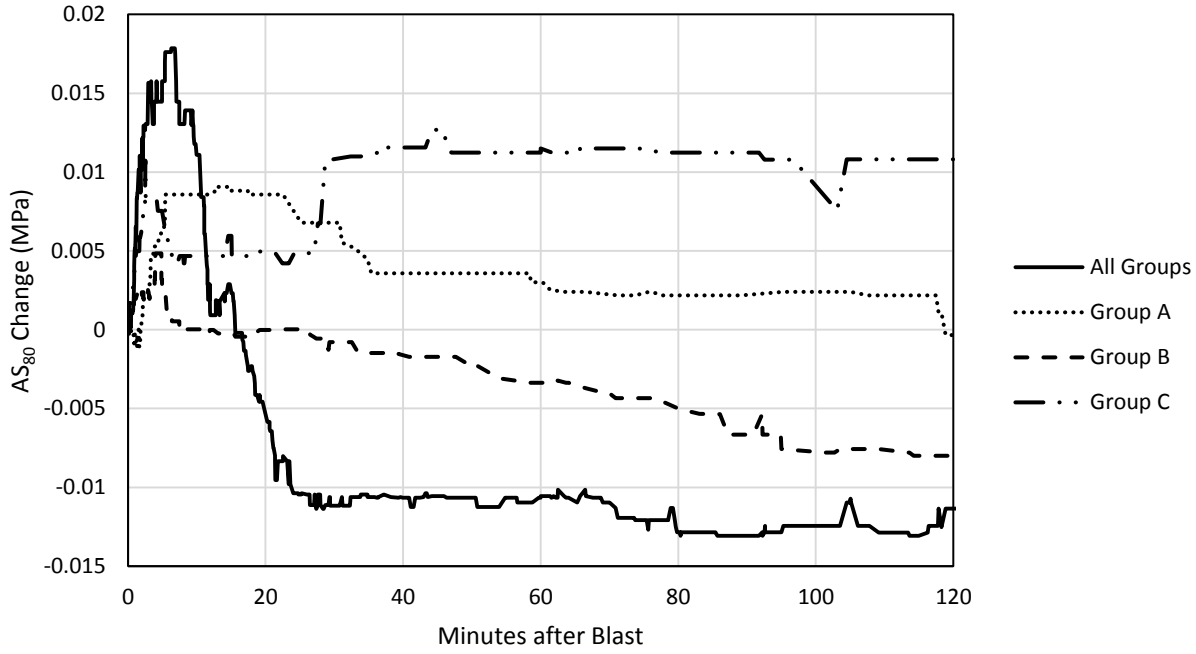

Figure 10 Changes in AS_{80} for spatially filtered groups around a stope blast

A possible interpretation of this behaviour is that the ground in group A experienced a stress increase as the overcut was daylighted and stresses were forced into the newly created stope back. The ground immediately above the back began to yield, corresponding with a drop in Log(EI) and AS_{80}. Group B's events are located close to the stope walls which have relatively low confinement. This volume might have little capacity to maintain a stress increase, so yield was more immediate. Group C's events are located farther from the stope than events in the other groups. The ground immediately adjacent to this side of the stope may be more damaged than other areas from earlier stope blasts. The events in group C may have occurred in more confined or intact ground. The blast may have increased stress in this area, which could not readily yield and shed stress.

From this example, we can also see how distinct spatial groups can dictate the overall trend in Log(EI) or AS_{80}. The initial increase in both trends might be driven by events in groups A and C. However, more events occurred in group B, and these events had initially lower EI and σ_a than the other groups. Therefore, the longer term decrease in both trends might be driven by behaviour in a spatially isolated area around the stope. This example shows how rock mass response cannot always be simplified to a uniform behaviour around an entire excavation.

4.2 Influence of strong events on trends

Static stress change from large seismic events can induce or trigger additional events. This phenomena has been observed in both natural (King et al. 1994) and mining (Orlecka-Sikora 2010) environments. The events that follow the initial large event may interrupt a trend in EI or σ_a, if there are enough of them, and if their source parameters are sufficiently different from the preceding events. The subsequent events may indicate how stress is changing following the large event. The following example shows one such case in which a M_w 1.9 event occurred approximately 18 hours after a 25,000 tonne stope blast. The location of the event is shown in Figure 11. The delayed large event occurred near the periphery of a cluster of events that occurred immediately following the blast. The smaller events that occurred after the large event were also outside the initial cluster, but extended along a planar trend 40 m deeper into the hanging wall which implies a structure-related mechanism for the delayed events.

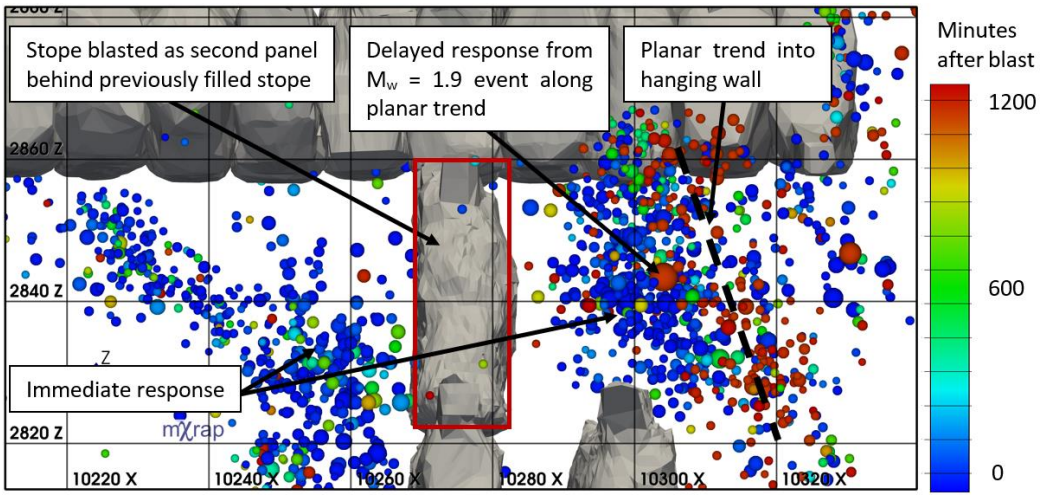

Figure 11 Longitudinal view of events following a stope blast with a large delayed response, events are coloured by time and sized by magnitude

The trends in Log(EI) and AS_{80} following the blast and large event are shown in Figure 12. The event occurred after a drop in both EI and σ_a between 600 and 1,000 minutes after the blast. It is not known if this drop is a precursor to the large event or an unrelated rock mass behaviour. The large event and subsequent smaller events were associated with a rapid increase in Log(EI) and AS_{80} that peaked after 20 minutes, followed by a slow decrease over the next 60 minutes. Although the temporal correlation between the blast and large event is weak, the location of the delayed events implies that they were triggered by a stress increase in the abutment following the blast. This example demonstrates how the smaller events that follow a large event may indicate the stress change occurring as a result of the large event. If a large enough event or series of large events occurs sooner after a blast, say within the first 10 minutes, trends in EI and σ_a may be more representative of the stress change from the large event(s) than the blast itself. Such effects may be more obvious when analysing seismic responses to development blasts rather than stope blasts. The voids created by development blasts are two orders of magnitude smaller than stope blasts, so the static stress change produced by a large event may be much greater relative to the induced stress change from a smaller blast. As a result, the subsequent events might imply a larger stress change or different pattern in stress change than one would expect from a small blast.

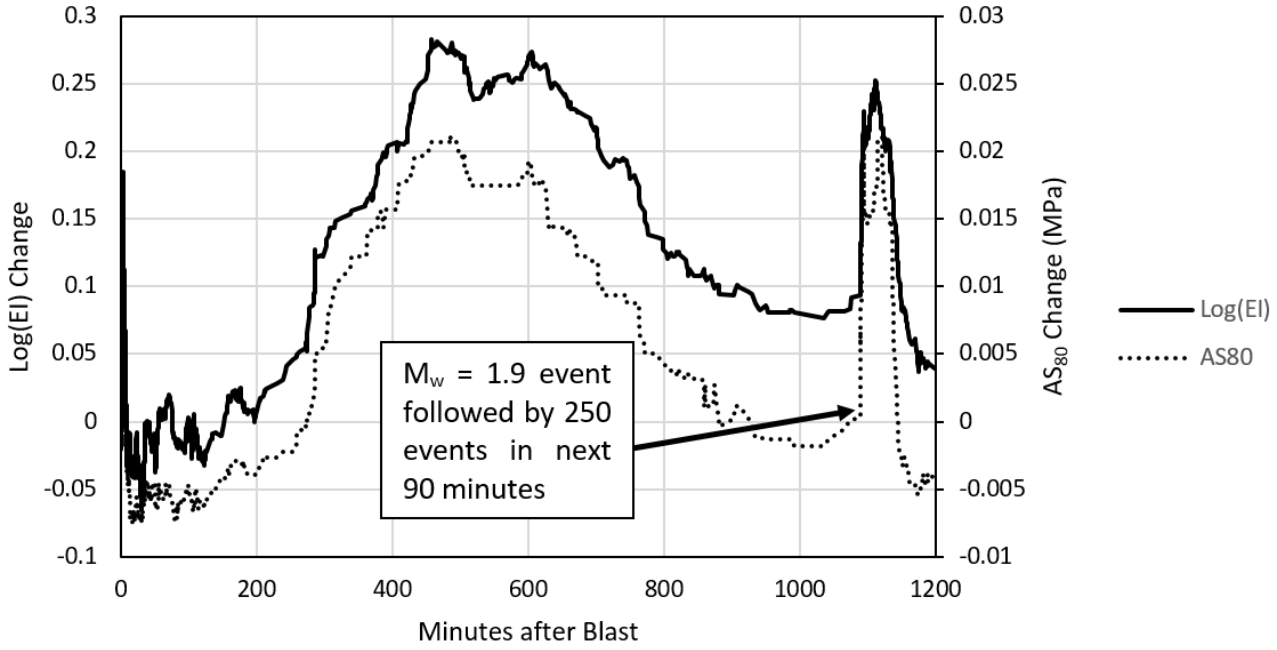

Figure 12 Trends in Log(EI) and AS_{80} after a stope blast and a delayed M_w = 1.9 event

5 Discussion

The trends in Log(EI) and AS_{80} in over 80% of the analysed cases show similar behaviour to Figure 4. The timing of relative co-seismic stress change increases and decreases in these cases are similar to those taken from a strain cell in yielding ground close to an open stope (Figure 1(b)). These similarities indicate that relative co-seismic stress change might correlate with stress in the rock mass as the ground loads and yields following stope blasts. It is postulated that the phases of relative stress change represent the following rock mass behaviour in the immediate hours after a blast:

- Phase 1: rapid stress increase in the immediate minutes following the blast.
- Phase 2: gradual stress decrease as the rock mass around the stope yields and sheds stress over the next hour(s).
- Phase 3: gradual stress increase in ground farther away from the stope that is more intact and/or confined.

The frequent observation of this pattern might be a result of the cases analysed. Stope blasts with the greater number of events were selected because more data was available for analysis. If we assume that a greater number of seismic events is a result of a greater amount of rock mass yield, then the results might indicate that inferred significant yielding responses are common simply because the rock mass underwent significant yield in the majority of analysed cases. Comparing the responses based on the cumulative seismic moment, a proxy for co-seismic deformation, might reveal interesting contrasts in Log(EI) and AS_{80} trends between blasts that induced more events, but less cumulative moment and blasts that induced fewer events, but more cumulative seismic moment. Furthermore, blasthole open stopes involve the creation of large voids and significant loss of confinement near stope walls. Blast size, mining geometry and sequence, stress, and rock mass properties all play a role in rock mass yield and seismic source mechanisms. Performing similar analysis at different mines may therefore reveal different trends and interpretations of rock mass yield.

Inferring stress changes based on seismic events within a volume assumes some degree of consistency in rock mass behaviour throughout that volume. The trends in relative co-seismic stress change, and our corresponding interpretation of rock mass behaviour drawn from them, will always be driven by the seismic source mechanisms and volumes of rock generating the most events. If there is uniformity in relative co-seismic stress change and the number of events through the volume, it might be fair to assume consistent rock mass behaviour throughout that volume. However, the example in Section 4.1 demonstrated that multiple trends and corresponding interpretations of rock mass behaviour can be found within spatially constrained volumes around a stope. Trends in EI and σ_a over larger volumes with varied rock mass properties, stress conditions, failure mechanisms, etc. will vary depending on:

- Where/when events occur.
- The number of events occurring at a given location/time.
- How drastically different EI or σ_a are at a given location/time compared to the others.
- Consistency of increase/decrease in either parameter.

Each of the aforementioned factors will influence how a subset of related events may dominate an overall trend. A greater quantity and quality of data will increase the resolution at which we can interpret stress change from seismic events, and reduce the number of assumptions that need to be made in order to infer localised behaviour.

Trends may also be influenced by scale dependence. If EI or σ_a does not vary uniformly for large and small events, a single measure of central tendency or distribution may misrepresent how relative stress change is varying for large or small events. Trends in scale-dependent parameters, such as apparent stress in this dataset, can also be influenced by the proportion of large and small events. The proportion of large and small events is somewhat correlated spatially and temporally with stress release estimates of seismic events (Urbancic et al. 1992). Therefore, Log(EI) and AS_{80} trends may be driven by variations in the proportions of large and small events, rather than purely a variation in radiated energy for events of all sizes.

The influence of the size of the moving windows for Log(EI) and AS_{80} computation was not investigated in detail. Generally speaking, the appropriate length of the moving window is dictated by the intent of the analysis. Shorter windows make the magnitude of increases and decreases more evident, but are inevitably noisier and give a lesser degree of statistical confidence in the values read from them at any given time. Longer windows can hide short-term variations, but provide more statistical confidence and may improve inferences of initial levels of stress before a blast. This study was focused on short-term variations, so a short moving window was chosen. The minimum and maximum sizes of a moving window that remain relevant and reliable for short-term analysis of co-seismic stress change may be a topic for future studies.

The relation between seismic hazard and trends in Log(EI) and AS_{80} is also of interest. Relating seismic hazard to a physical rock mass response may give insight into how yield and stress readjustment relates to the occurrence of large events. The trends may also distinguish themselves from other re-entry protocols that are based on frequencies of events or seismic energy or moment release.

6 Conclusions

Moving trends of Log(EI) and AS_{80} folllowing stope blasts show similarities to measurements from strain cells. These similarities may make these seismic source parameters potentially valid and meaningful indicators of stress increase and decrease in a yielding rock mass. A significant yielding response can be inferred from the majority of analysed cases in this study. The large number of yielding responses may be a result of analysing blasts that induced a large number of events or by local site characteristics such as the rock mass properties or stope sizes. However, spatial filtering also affects the results of the analysis, as individual spatial groups around a stope can show different degrees of relative co-seismic change increase or decrease over time. The examples presented in this study demonstrate how analysis of seismic source parameters can provide useful information on the response of the rock mass to mining, and help mines gain more value from their seismic monitoring systems as a practical ground control tool.

Acknowledgement

The authors acknowledge the financial support of the sponsors of the Data Driven Seismic Hazard Evaluation in Canadian Mines project: Agnico Eagle, KGHM, Vale, the Australian Centre for Geomechanics, and the Natural Sciences and Engineering Research Council of Canada. The authors also thank Glencore for allowing the publication of this paper and anonymous reviewers, whose comments significantly improved this paper.

References

Alcott, JM, Kaiser, PK & Simser, BP 1998, 'Use of microseismic source parameters for rockburst hazard assessment', *Pure and Applied Geophysics*, vol. 153, no. 1, pp. 41–65.

Aki, K & Richards, PG 1980, *Quantitative Seismology: Theory and Methods*, Freeman, San Francisco.

Brown, LG 2015, *Seismic Hazard Evaluation Using Apparent Stress Ratio for Mining-Induced Seismic Events*, MSc Thesis, Laurentian University, Sudbury.

Brown, L & Hudyma, M 2017a, 'Identification of stress change within a rock mass through apparent stress of local seismic events', *Rock Mechanics and Rock Engineering*, vol. 50, no. 1, pp. 81–88.

Brown, L & Hudyma, M 2017b, 'Identifying local stress increase using a relative apparent stress ratio for populations of mining-induced seismic events', *Canadian Geotechnical Journal*, vol. 54, no. 1, pp. 128–137.

Glazer, SN & Hepworth N 2006, 'Crown pillar failure mechanism – case study based on seismic data from Palabora Mine', *Mining Technology: Transactions of the Institutions of Mining and Metallurgy: Section A*, vol. 115, no. 2, pp. 75–84.

Harris, PC & Wesseloo J 2015, *mXrap*, version 5, Australian Centre for Geomechanics, Perth, viewed 7 July 2017, http://www.mxrap.com/

Hudyma, MR 2008, *Analysis and Interpretation of Clusters of Seismic Events in Mines*, PhD Thesis, The University of Western Australia, Perth.

Hudyma, MR, Potvin, Y, Grant, DR, Milne, D, Brummer, RK & Board, M 1994, 'Geomechanics of sill pillar mining', in PP Nelson & SE Laubach (eds), *Proceedings of the 1st North American Rock Mechanics Symposium*, A.A. Balkema, Rotterdam, pp. 969–976.

Ide, S & Beroza, GC 2001, 'Does apparent stress vary with earthquake size?', *Geohpysical Research Letters*, vol. 28, no. 17, pp. 3349–3352.

King, GCP, Stein, RS & Lin, J 1994, 'Static stress changes and the triggering of earthquakes', *Bulletin of the Seismological Society of America*, vol. 84, no. 3, pp. 935–953.

Mendecki, AJ, van Aswegen, G & Mountfort, P 1999, 'A guide to routine seismic monitoring in mines', in AJ Jager & JA Ryder (eds), *A Handbook on Rock Engineering Practice for Tabular Hard Rock Mines*, Creda Communications, Cape Town.

Orlecka-Sikora, B 2010, 'The role of static stress transfer in mining induced seismic events occurrence, a case study of the Rudna mine in the Legnica-Glogow Copper District in Poland', *Geophysical Journal International*, vol. 182, no. 2, pp. 1087–1095.

Simser, B & Falmagne, V 2004, 'Seismic source parameters used to monitor rockmass response at Brunswick mine', *CIM Bulletin*, vol. 97, no. 1080, pp. 58–63.

Syrek, B & Kijko, A 1988, 'Energy and frequency distribution of mining tremors and their relation to rockburst hazard in the Wujek coal mine, Poland', *Acta Geophysica Poland*, vol. 36, no. 3, pp. 189–201.

Urbancic, TI, Trifu, C-I, Long, JM & Young, RP 1992, 'Space-time correlations of b-values with stress release', *Pure and Applied Geophysics*, vol. 139, no. 3–4, pp. 449–462.

van Aswegen, G & Butler, AG 1993, 'Applications of quantitative seismology in South African gold mines', in RP Young (ed.), *Proceedings of the 3rd International Symposium on Rockbursts and Seismicity in Mines*, A.A. Balkema, Rotterdam, pp. 261–266.

Wesseloo, J, Woodward, KR & Pereira, J 2014, 'Grid-based analysis of seismic data', *Journal of The South African Institute of Mining and Metallurgy*, vol. 114, no. 10, pp. 815–822.

Wyss, M & Brune, JN 1968, 'Seismic moment, stress, and source dimensions for earthquakes in the California-Nevada Region', *Journal of Geophysical Research*, vol. 73, no. 14, pp. 4681–4694.

Young, DP 2012, *Energy Variations in Mining-Induced Seismic Events Using Apparent Stress*, MSc Thesis, Laurentian University, Sudbury.